Annals of Biomedical Engineering (© 2023)
https://doi.org/10.1007/s10439-023-03139-8

BMES BIOMEDICAL ENGINEERING SOCIETY

Original Article

The Use of Collagen Methacrylate in Actuating Polyethylene Glycol Diacrylate–Acrylic Acid Scaffolds for Muscle Regeneration

Yoliem S. Miranda Alarcón, Dorota Jazwinska, Terrence Lymon, Amin Khalili, Daniel Browe, Brandon Newton, Michael Pellegrini, Rick I. Cohen, David I. Shreiber, and Joseph W. Freeman

Department of Biomedical Engineering, Rutgers University, Piscataway, NJ 08854, USA

(*Received 25 May 2022; accepted 3 January 2023*)

Associate Editor Elizabeth Cosgriff-Hernandez oversaw the review of this article.

Abstract—After muscle loss or injury, skeletal muscle tissue has the ability to regenerate and return its function. However, large volume defects in skeletal muscle tissue pose a challenge to regenerate due to the absence of regenerative elements such as biophysical and biochemical cues, making the development of new treatments necessary. One potential solution is to utilize electroactive polymers that can change size or shape in response to an external electric field. Poly(ethylene glycol) diacrylate (PEGDA) is one such polymer, which holds great potential as a scaffold for muscle tissue regeneration due to its mechanical properties. In addition, the versatile chemistry of this polymer allows for the conjugation of new functional groups to enhance its electroactive properties and biocompatibility. Herein, we have developed an electroactive copolymer of PEGDA and acrylic acid (AA) in combination with collagen methacrylate (CMA) to promote cell adhesion and proliferation. The electroactive properties of the CMA + PEGDA:AA constructs were investigated through actuation studies. Furthermore, the biological properties of the hydrogel were investigated in a 14-day *in vitro* study to evaluate myosin light chain (MLC) expression and metabolic activity of C2C12 mouse myoblast cells. The addition of CMA improved some aspects of material bioactivity, such as MLC expression in C2C12 mouse myoblast cells. However, the incorporation of CMA in the PEGDA:AA hydrogels reduced the sample movement when placed under an electric field, possibly due to steric hindrance from the CMA. Further research is needed to optimize the use of CMA in combination with PEGDA:AA as a potential scaffold for skeletal muscle tissue engineering.

Keywords—Muscle tissue engineering, Electroactive polymers, Collagen methacrylamide.

Address correspondence to Joseph W. Freeman, Department of Biomedical Engineering, Rutgers University, Piscataway, NJ 08854, USA. Electronic mail: joseph.freeman@rutgers.edu

INTRODUCTION

Skeletal Muscle accounts for 40% of human body weight and is important locomotion, maintaining posture, and regulating body temperature. Some of the major morbidities associated with skeletal muscle tissue include trauma, progressive diseases, and aging.[15] Skeletal muscle can also be impaired by diseases, such as myasthenia gravis (MG) and Duchenne muscular dystrophy (DMD). These conditions lead to muscle weakness and even death.[42,44,59,60,71,73] Approximately 5.6 million people in the U.S. are paralyzed and stroke leaves 1.6 million people in a weakened state[27]; these patients lack muscular damage but have lost muscular function.

The body attempts to repair damaged muscle by removing necrotic muscle fibers and activating satellite cells to regenerate muscle.[3] However, satellite cell incidence in the tissue is extremely low, approximately 1–5%, and dependent on age and muscle fiber composition.[3] One of the methods used to replace muscle tissue from a region of the body experiencing significant loss is by taking muscle tissue from other parts of the body for implantation.[44] This is viable for small muscular defects but not large-scale losses, it also introduces the potential for donor site morbidity. Intramuscular injections of skeletal myoblasts have shown little effect due to inadequate distribution and low cell survival rate.

Researchers have investigated a variety of materials and techniques for this purpose. Many research groups have used hydrogels for skeletal muscle tissue engineering. Some of the materials used in recent hydrogel

Published online: 28 February 2023

development include blends of Collagen,[31,34,58,64] Gelatin,[18,25] Chitosan,[28] Alginate,[6,26,62] Hyaluronic Acid,[46,72] Chondroitin Sulphate,[41] Silk Fibroin,[7,10] Fibrin gels,[58,65] and Methacrylated Gelatin (GelMA).[22,50] In a study conducted by Pollot *et al.* it was shown that Fibrin exposure to precursor cells lead to the highest expression of genes for myotube development for days 7 and 14.[56] Other composites mixed of Collagen, Chitosan, and Fibrin were shown to have optimal elasticity for driving muscle differentiation. In other studies Arginine, Glycine and Aspartic acid linked as external motifs have been shown to support myoblast growth.[37,45] The use of gel methacrylates crosslinked using UV light have offered new versatility in terms of 3D bioprinting, encapsulation, and casting of myoblasts with specialized topographical cues.[49] Skeletal muscle is electrically active due to the movement and some level of electrical stimulation is synergistic to accelerating muscle differentiation.[33,55,70] Conductive gels can be used to electrically stimulate cells for the reformation of tissue. Some of the materials used for this purpose include graphene oxide,[29,53] Polyethylene glycol fused with poly(3, 4-ethylenedioxythiophene) (PEDOT),[24] graphene polyacrylamide,[29,53] polypyrrole nanoparticles in type I collagen—chondroitin sulphate,[24] and mixtures of the aforementioned.

In addition, biodegradable thermoplastic polymers such as polycaprolactone have been fabricated into scaffolds for the support of myoblasts.[2,74,75] Poly(lactide *co*-glycolide) electrospun mats have been used in the alignment of myoblasts and in a study conducted by Narayanan *et al.*, myoblasts were implanted on these mats and further implanted into a mouse model which showed improved integration of tissue over controls.[47,51,52] In another study, Patel *et al.* mixed polycaprolactone with decellularized muscle tissue and found an increase in myoblast density over controls and in a follow up study showed myofiber generation in a mouse model with large scale muscle loss.[54]

A major area in skeletal muscle tissue engineering is the use of decellularized matrices. This technique has been seen a great deal of interest in the area of large volume muscle loss. It has been demonstrated that the implementation of vascularized cells (human umbilical vein endothelial cell) in these scaffolds increased expression of factors for myotube formation.[74,75] Other groups have examined the utility of implanting decellularized muscle tissue directly into a muscle defect which has proven to drive angiogenesis, myoblast and satellite cell migration and muscle regeneration *in vivo*.[54,57,76] Decellularized muscle tissue can also be formulated into hydrogels[66,67] and bioinks.[13,14,17,32] A recent study examined the 3D printing of cell infused decellularized bioinks and found that the process allowed for high cell viability after muscle loss within a rat model.[13] Modifying decellularized skeletal muscle with methacrylate to manufacture photocross-linkable hydrogels allows for stiffness fine tuning as well as increased longevity.[35]

In addition to a variety of materials, skeletal muscle cells have been grown *in vitro* under a variety of culture conditions. Mechanical strain or electrical stimulation have also been used to improve muscle utility after regeneration. Studies have shown that mechanical and electrical stimulation of myoblasts lead to more mature muscle fibers with better contractility.[3,16,20,38]

A potential tissue-engineered solution for large volume muscle loss may include electroactive polymers (EAPs); ionic EAPs have been investigated as robotic actuators.[5] Ionic EAP actuation is caused by ion displacement inside the polymer.[4,48] A few volts are required, but the ionic flow implies a higher electrical power for actuation[5]; examples include ionomeric polymer–metal composites (IPMCs). They are usually layered with a conductive layer (metal or conductive polymer), followed by an EAP layer and another conductive layer. When activated, the gels bend as the cathode side becomes more alkaline and the anode side more acidic, and ions diffuse through the gel. IPMCs can actuate and match biological muscle forces.[4] They are flexible, compliant, fast responding, and lightweight.[40] Poly(ethylene glycol) diacrylate (PEGDA) combined with acrylic acid (AA), functions as an EAP network. PEGDA is a well-characterized scaffold for a number of possible uses in tissue engineering due to its mechanical properties.[43] This polymer combined with AA, affords an EAP network, which can actuate when an electric field is applied to it. PEGDA:AA holds promise in utilization for muscle regeneration in conjunction with myoblast cells.[8] However, as the concentration of AA goes up, it lowers the pH of the media which the cells are in, resulting in an unfavorable environment for cellular growth and differentiation.[8] Additionally, the cells implanted in the PEGDA:AA constructs fail to form long linear myotubes, more than likely due to the lack of guidance cues and low attachment.[8]

Collagen type I is a greatly utilized scaffold in tissue engineering due to its self-assembling abilities to afford a fibrillar structure that contributes to characteristics such as biocompatibility, biodegradability, and promotion of cellular adhesion.[23] Chemical alterations can also be made due to its chemical versatility to help control the mechanical properties of collagen; one such material is collagen methacrylate (CMA).[19] The covalent attachment of methacrylic acid allows for the collagen to become photocross-linkable through the mediation of UV light and a free-radical source, allowing for additional manipulation of this biomate-

rial.[19] Furthermore, CMA can crosslink to moieties susceptible to polymerization such as acrylates. CMA can be rapidly crosslinked with spatial control.[19,23] Photocrosslinked CMA shows lower degradation rates than uncrosslinked CMA and native collagen, which is beneficial when using the material as a scaffold.[23] Due to its retention of native collagen features and addition of new characteristics, CMA can be utilized for tissue engineering, drug delivery, cellular encapsulation, and microenvironment studies.[12,19] Peer-reviewed studies have shown improved cell viability when supplementing synthetic and organic polymers with collagen-based biomaterials such as CMA, as well as its denatured form, gelatin methacrylamide (gelMA) to develop hydrogels for applications in muscle tissue engineering.[36,69] This is due to collagen's cytocompatibility conferred by the innate and complex chemical structure that fosters cell-to-cell interactions and the protein's prevalence in muscle tissue engineering.[12]

The favorable properties of PEGDA:AA causing actuation when stimulated with electricity and the ability of CMA to be manipulated and support cellular growth hold much promise in creating a construct utilizing both for muscular regeneration. Collagen has been used to culture myoblasts to promote differentiation, provide a guidance matrix for long myotube development, cellular migration, and accelerate myotube maturation.[9,18,19] Utilizing CMA provides all the same cellular cues which help with the myoblast differentiation and myotube formation, with the added benefit of crosslinking and reduced degradation.[19] CMA is able to crosslink with the AA of the PEGDA:AA network under UV light exposure. The CMA + PEGDA:AA construct will provide a biocompatible environment for myoblast differentiation, contact guidance provided by the CMA to grow long myotubes, and ability to respond to electrical stimulus.

In this study, we describe the fabrication of a biocompatible, electroactive hydrogel, consisting of PEGDA:AA and CMA, which actuates in an electric field. Previous work demonstrated that a PEGDA:AA ratio of 1:4 presented the highest metabolic activity and matrix deposition, while a ratio of 1:8 showed the highest actuation response.[8] Thus, this study will focus on PEGDA:AA 1:4 and 1:8 compositions. The mechanical, biological, and electroactive properties of this interpenetrating network are further characterized *in vitro*. We hypothesize that the addition of CMA will improve the cellular microenvironments of the PEGDA:AA constructs through the chemical cues presented by the collagen backbone of CMA, which in turn will promote cell adhesion and proliferation.

Stimulus-responsive biomaterials have shown promise in developing muscle tissue constructs. In particular, ionic EAPs based on PEGDA allow for high control and specificity of the chemical structure with superior swelling capacity.[8,63] The use of PEGDA presents limited biocompatibility posing a challenge to developing constructs that promote cell growth and proliferation. In this paper, we introduce the use of collagen methacrylamide (CMA) to improve scaffold biocompatibility and bioactivity of PEGDA constructs. As a collagen derivative, CMA promotes cell adhesion and proliferation, while preserving collagen's unique chemistry to spontaneously self-assemble and degrade enzymatically. We aim to develop a biocompatible material that reversibly contracts in an electric field and encourages myoblast growth and differentiation.

MATERIALS AND METHODS

PEGDA:AA Hydrogel Crosslinking

Poly(ethylene glycol) diacrylate (PEGDA) with molecular weights of 10,000 Da were purchased from Monomer-Polymer and Dajac Labs (an MPD Chemicals Company). AA monomer (anhydrous), 2, 2-Dimethoxy-2-phenylacetophenone, 1-vinyl-2-pyrrolidinone, and phosphate buffered saline (PBS) were purchased from Sigma Aldrich. PEGDA was combined with different amounts of AA to obtain a ratio of 1:4 and 1:8.[8] All hydrogel solutions were prepared by dissolving PEGDA and AA in PBS using a vortex mixer. To prepare the photoinitiator solution, 2, 2-dimethoxy-2-phenylacetophenone was mixed in 1-vinyl-2-pyrrolidinone, and 50 μL of the solution were added per 1 mL of hydrogel solution at 5% (w/v) prior to UV exposure. The photoinitiator and hydrogel mix were injected into a pre-assembled glass mold with a rectangular prism shape. The injected mold was exposed to UV radiation at a 365 nm wavelength using a 3UV™ lamp (UVP: Ultra-Violet Products S/N 100306-001, P/N 95-0343-01; 8 W Upland, CA, USA) in 30 s intervals until the hydrogel solution solidified. UV radiation, in the presence of a photoinitiator and acrylate groups, causes free-radical polymerization affording a random 3D polymer network. After UV exposure, the dimensions of the hydrogel were taken (diameter and thickness). The hydrogel samples were soaked in PBS for 3 days to achieve maximum swelling.

CMA Synthesis

The detailed synthesis can be found in Gaudet and Shreiber.[23] Type-I collagen extracted from bovine skin (C857, Telo-EPC) was obtained from Elastin Products (Owensville, MO). All other reagents were purchased

from Sigma. Briefly, collagen type-I was modified by reacting the free amines of lysine residues with methacrylate groups to create collagen methacrylamide (CMA). 1-ethyl-3-(3-(dimethylamino)propyl) carbodiimide EDAC and *N*-hydroxysuccinimide (NHS) in MES buffer were used to activate the carboxylic acid in methacrylic acid. Collagen at 3.75 mg/mL in 0.02 N acetic acid was added to this mixture to form CMA. CMA was dialyzed, lyophilized, and reconstituted in 0.02 N acetic acid. Derivatization efficiency was evaluated using fluorescamine, a molecule that fluoresces when it binds to primary amines. Native type-I collagen that was not reacted with methacrylic acid was used as a standard curve to assess the percentage of modified lysines in collagen type-I. Soluble fluorescamine (3 mg/mL) was added to a collagen type-I standard curve and CMA samples, and the fluorescence intensity was read with an excitation wavelength of 400 nm and emission wavelength of 460 nm. The synthesized material showed a 40.4% degree of derivatization from unmodified collagen type-I.

Hydrogel Preparation

PEGDA:AA hydrogels were cut to a diameter of 1 cm with thickness of 0.3–0.4 mm to fit inside a 24-well plate and sterilized by rinsing them in ethanol and applying UV radiation for 30 min on each side ($n = 6$). This was followed by a wash with sterile PBS before soaking overnight in DMEM media with 10% fetal bovine serum (FBS) and 1% penicillin/streptomycin (P/S).

CMA + PEGDA:AA hydrogels were prepared by coating PEGDA:AA hydrogels with 200 μL of buffered CMA in a pre-design setup using a glass slide with a mold thickness of 0.75 mm to allow for UV crosslinking and a polydimethylsiloxane (PDMS) ring with a diameter of 1.1 cm to hold the hydrogel volume in place. Briefly, CMA was buffered on ice according to the following formula: 20 μL 1 M HEPES (H3537, Sigma-Aldrich, St. Louis, MO), 44 μL 0.15 N NaOH (S2770, Sigma-Aldrich), 100 μL 10 × PBS (P5493, Sigma-Aldrich), 149 μL 1 × PBS (860454, Thermo Fisher Scientific, Waltham, MA), 10 μL 10% Irgacure (I2959, a gift from Ciba Specialty Chemicals) solubilized in neat methanol, and 677 μL CMA at 3.75 mg/mL. CMA + PEGDA:AA hydrogels were self-assembled for 1 h at 37 °C. The hydrogels were photocrosslinked using UV light (365 nm, 50 mW/cm^2) for 120 s. After UV crosslinking, CMA + PEGDA:AA hydrogels were rinsed with warm media (1 mL) to remove any reaction byproducts from photocrosslinking. The engineered CMA + PEGDA:AA hydrogels, afforded a middle layer of PEGDA surrounded by CMA with uniform thickness and no interface between both materials.

Actuation Studies

Several formulations of PEGDA:AA were made by altering the volumes of PEGDA and AA used. 1:4 PEGDA:AA, 1:8 PEGDA:AA, CMA + 1:4 PEGDA:AA, and CMA + 1:8 PEGDA:AA hydrogel samples ($n = 4$) were cut into 20 mm × 4 mm strips. The actuation testing device, used to study the response of each hydrogel to an electric field, as described in Browe *et al.*, consisted of a 150 mm × 15 mm polystyrene Petri dish (P5981, Sigma) with two pegs attached in the middle of the platinum electrodes placed in the center of the dish 3.0 cm apart from each other and submerged in PBS.[8] The platinum electrodes included four twisted platinum wires (99.5% pure) with a 0.20 mm diameter. The hydrogel strips were suspended in PBS and placed in the center between two pegs (Fig. 1). A DC voltage of 20 V or 6.67 V/cm was applied in two 1-min intervals on each direction (two cycles of + for 60 s followed by − for 60 s) using an Agilent Dual Output DC Power Supply (E3646A Agilent Technologies, Santa Clara, CA, USA). This afforded a total of 4 min of stimulation per hydrogel strip. Each actuation study was recorded using a digital video camera. The videos were analyzed to determine the angular movement of the hydrogel strip during actuation. The obtained results are reported as the average and standard deviation of the change in angle.

Cell Line Development and Evaluation

A reporter cell line was developed by transducing the myosin light chain (MLC) promoter with the luciferase gene into C2C12 cells. A plasmid was designed with the DNA of the MLC promoter and the luciferase gene along with resistance to Blasticidin. This plasmid was generously gifted to our lab by Dr. Emmanuel Ekwueme and Dr. Craig Neville from Massachusetts General Hospital-Harvard Medical School. The plasmid was packaged into a lenti-virus and transduced into C2C12 myoblasts with the help of 1 μg/mL Polybrene. After 3 days in culture, the transduced cells were selected using media with 2 μg/mL Blasticidin changed every other day for a week. The surviving cells were grown up and frozen down for later use.

In order to validate the cell line development, the transduced MLC reporting C2C12 myoblasts were seeded in 12-well plates at a density of 25,000 cells/cm^2 (purchased from ATCC). Three different groups ($n = 4$) were compared: (1) cells supplemented with 50 ng/mL IGF-1 meant to enhance myoblast differ-

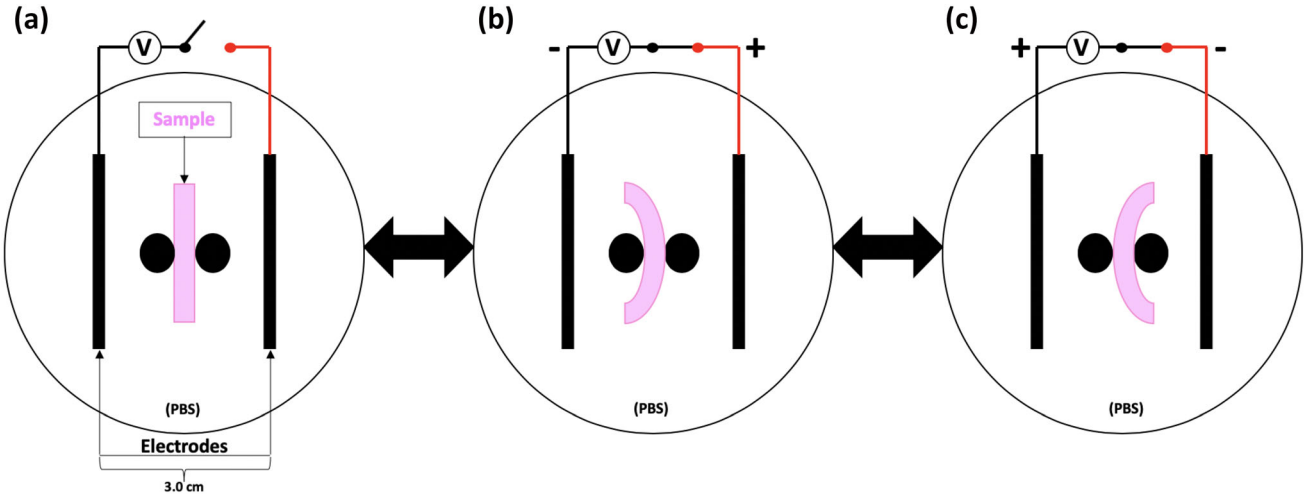

FIGURE 1. Actuation study device layout (top view shown above). The devices in PBS baths had 20 V of DC voltage applied across the hydrogel strips from two platinum electrodes 3.0 cm apart. (a) Samples held in place by two small pegs on either side to immobilize during testing. (b) Sample bends toward negative electrode when voltage is applied. (c) When polarity voltage is reversed, sample bends in opposite direction.

entiation, (2) cells supplemented with 40 μg/mL dexamethasone meant to deter myoblast differentiation, and (3) cells fed with the base media without any additives meant as a null control. During the initial proliferation phase (day 0 to day 2), all groups were fed with a base media of DMEM media with 10% FBS and 1% P/S every other day. During the differentiation phase (day 3 to day 10), all samples were fed with a base media of DMEM media with 1% FBS and 1% P/S with the corresponding additives appropriate for each group once per day.

A luciferase assay was performed at 1, 3, and 7 days after differentiation media was initially applied with a BioLux® Gaussia Luciferase Assay Kit (New England Biolabs, Ipswich, MA) according to the manufacturer's instructions. After the last time-point, all groups were fixed with a 4% paraformaldehyde solution to prepare for staining ($n = 4$). Cells were stained with NucBlue® fixed cell ReadyProbes® reagent (Thermo Fisher Scientific) for DNA (Blue) and Fluorescein Phalloidin (Thermo Fisher Scientific) for F-actin (Green).

A representative sample of five images for each group was used to quantify the morphology of the cells in the different groups. ImageJ software [version 1.46r/Java 1.6.0_25 (32-bit)] was used to quantify the total number of nuclei, the total number of myotubes, and the number of nuclei inside of myotubes for each image. Myotubes were defined as clearly distinguishable, linear structures which contained two or more nuclei. These parameters were used to calculate the fusion index (nuclei inside of myotubes/total number of nuclei).

CMA–PEGDA:AA Hydrogel Cell Study

C2C12 mouse myoblast cells were expanded in tissue culture flasks until 90% confluency in DMEM media (D5546, Sigma) with 10% FBS (S11550, Atlanta Biologicals, Flowery Branch, GA), and 1% P/S (P4458, Sigma-Aldrich). After expansion, C2C12 cells were detached using TripLE Express (12604013, Thermo Fisher), washed in culture media, and encapsulated in buffered hydrogel suspensions at 1,000,000 cells/mL.

Hydrogel samples were seeded with approximately 50,000 C2C12 cells and further incubated at 37 °C, 5% CO_2 for 14 days. Cells were seeded on top of the hydrogel. For the first 7 days, all wells were fed daily with DMEM media with 10% FBS and 1% P/S to encourage proliferation. From day 7 to day 14, all wells were fed daily with DMEM media with 1% FBS and 1% P/S to encourage differentiation. As a positive control, cells were seeded in tissue culture plastic and subjected to the same conditions.

To study metabolic activity and cellular attachment, a PrestoBlue® cell viability assay (Thermo Fisher Scientific) was carried out on days 3, 7, 10, and 14 ($n = 4$). Briefly, the media was removed from all wells and replaced with PrestoBlue® cell viability reagent diluted with media to a 1:10 ratio and incubated with cell-seeded hydrogels for 30 min. After incubation, the reagent was transferred into a 96 well plate and absorbance was read on a plate reader at 570 nm.

After the PrestoBlue® cell viability assay was carried out, a cytotoxicity study was performed using Live/Dead Viability/Cytotoxicity kit (L3224, Thermo Fisher Scientific). To assess cell viability at each time

point (days 3, 7, 10, and 14), each cellular hydrogel and TCP control was rinsed with PBS 3 times and calcein-AM (4 mM) and ethidium homodimer-1 (2 mM) were added and incubated for 30 min at room temperature. Following incubation, hydrogels and corresponding controls were imaged using an Olympus IX81 fluorescence microscope.

To measure gene expression of MLC a luciferase assay was carried out utilizing the Pierce™ Gaussia Luciferase Glow Assay Kit (Thermo Fisher Scientific). To prepare the working solution, 50 μL of 100 × Coelenterazine were mixed with 5 mL of Gaussia Glow Assay Buffer. After incubation, media was collected from cells on days 3, 7, 10, and 14 (n = 4). In a 96 well plate, 20 μL of media was combined with 50 μL of working solution before measuring luminescence on a plate reader.

On day 14, cells were fixed with a 4% paraformaldehyde solution and prepared for staining to visualize cell morphology and identify myotube fusion. Cells were stained with Alexa Fluor 488 Phalloidin (Thermo Fisher Scientific) and DAPI (Invitrogen), and imaged using an Olympus IX81 fluorescence microscope.

Image Analysis

Images were analyzed to determine the number of myotubes in each group to correlate with the luciferase data signifying myoblast differentiation into muscle tissue. Fusion index, a measure of myoblast differentiation, was determined for each group by counting the number of myotube nuclei and the number of total nuclei.[30,68] Myotube nuclei are defined as nuclei contained within a myotube containing at least three nuclei, indicated by a region of continuous and intense actin staining. Monochromatic images of the same area were processed to remove the background fluorescence by adjusting the minimum and maximum cutoff values for the grayscale image. The images were then merged using the color channel feature to obtain an overlay of the grayscale channels. Using the cell counter tool under the tools and macros tab the number of myotube nuclei were counted manually. In order to obtain the total nuclei the grayscale DAPI channel was thresholded using a mean threshold filter and eroded and dilated to remove small pixel noise, following the watershed operation we used to analyze particles to count the total number of nuclei. A minimum of three images were analyzed per group with some groups containing more images. All image analysis was performed using the Fiji distribution of ImageJ.

Statistics

The actuation and cellular analysis data gathered through this study underwent statistical analysis performed by two-way analysis of variance (ANOVA) with a Tukey's *post hoc* test and confidence level of 95% (α = 0.05) for statistical significance (denoted by *). Fusion index data was subjected to a one tailed t-test and a one-way ANOVA with a Tukey's *post hoc* test. Both the t-tests and ANOVA used an α = 0.05 for significance. All data was expressed as mean ± standard deviation.

RESULTS

Actuation Studies

During the actuation tests, all hydrogel samples exhibited reversible and repeatable movement when exposed to an electric field. A higher degree of movement in the forward direction was observed in the 1:8 PEGDA:AA (Fig. 3) compared to 1:4 PEGDA:AA (Fig. 2). We hypothesize that this is due to the presence of more AA, affording more anions. With more negatively charged ions there are more binding sites for water. The increase in water molecules bound to the hydrogel will improve hydrogel swelling, achieving more movement. The addition of CMA significantly reduces movement in the forward direction for 1:4 PEGDA:AA hydrogels (Fig. 2). However, CMA significantly inhibits movement when incorporated to 1:8 PEGDA:AA in both directions (Fig. 3). The CMA incorporated, given its viscous fluid nature before crosslinking made the samples non-homogeneous in shape.

CMA–PEGDA–AA Hydrogel Cell Study

Cell Studies

The results for the validation of the transduced MLC reporting C2C12 cell line with a luciferase assay are shown in Fig. 4. On day 1, the group exposed to dexamethasone had significantly lower MLC production than the control group. On days 3 and 7, the group exposed to IGF-1 was significantly higher than the control group and the dexamethasone group was significantly lower than the control group. Over time, MLC production increased in the control group, MLC production increased at a faster rate in the IGF-1 group, and MLC production decreased over time in the dexamethasone group.

The results for the morphological analysis of the myoblasts for the cell line validation are shown in Fig. 5. The number of myotubes produced and the

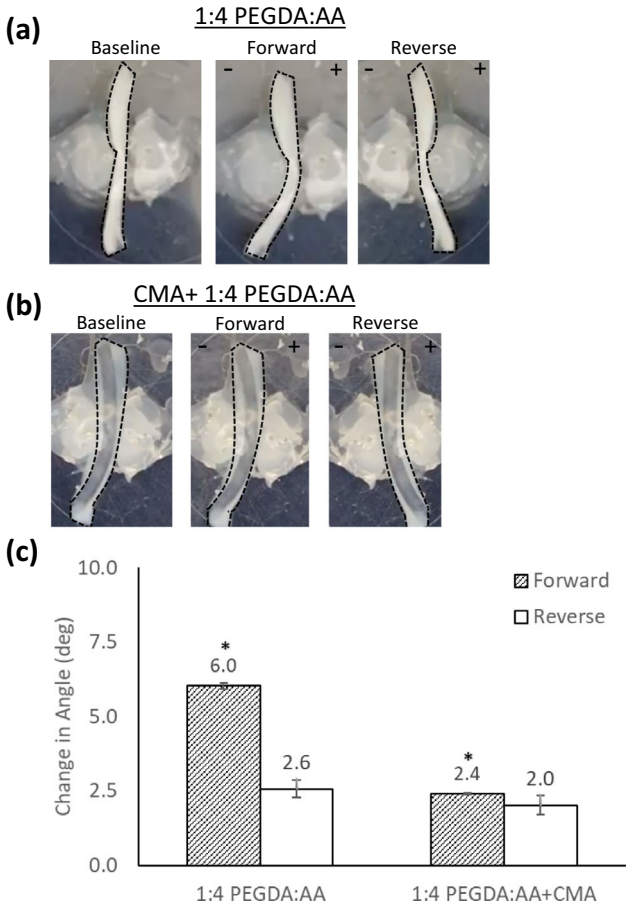

FIGURE 2. Effect of CMA on angular movement of 1:4 PEGDA:AA ($n = 4$). The movements in the forward and reverse directions are shown for both groups. A single factor ANOVA test was conducted for each statistical analysis test (*indicates a statistically significant difference between the conditions and corresponding movements). (a) Photographic representation of the 1:4 PEGDA:AA hydrogel during actuation studies. (b) Photographic representation of the 1:4 PEGDA:AA + CMA hydrogel during actuation studies. (c) Actuation result values presented as change in angle.

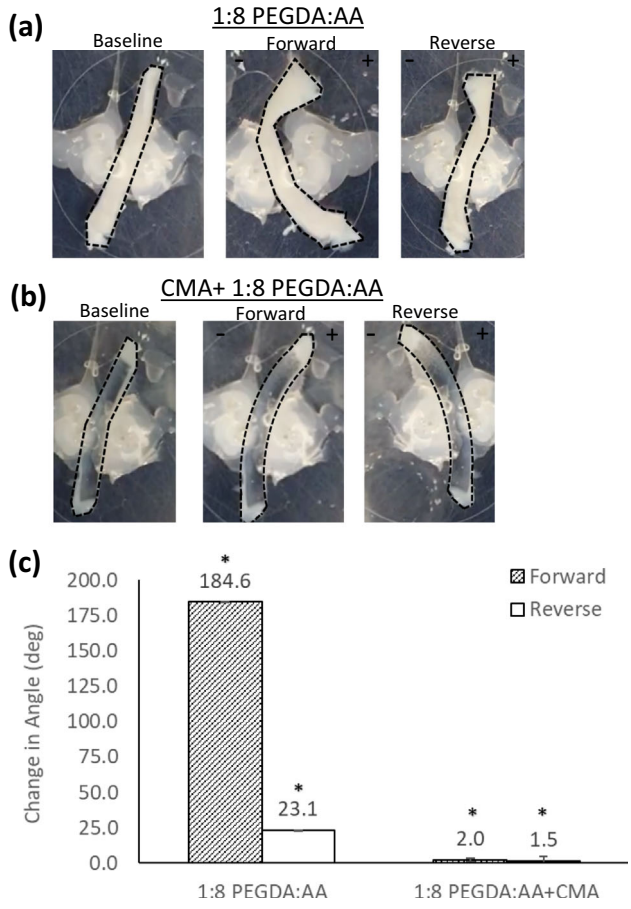

FIGURE 3. Effect of CMA on angular movement of 1:8 PEGDA:AA ($n = 4$). The movements in the forward and reverse directions are shown in both groups. A single factor ANOVA test was conducted for each statistical analysis test (*indicates a statistically significant difference between the conditions and corresponding movements). (a) Photographic representation of the 1:8 PEGDA:AA hydrogel during actuation studies. (b) Photographic representation of the 1:8 PEGDA:AA + CMA hydrogel during actuation studies. (c) Actuation result values presented as change in angle.

fusion index was significantly greater in the cells treated with IGF-1 as compared to the control. Dexamethasone completely blocked the formation of myotubes, resulting in zero myotubes and a zero fusion index. Overall, the results of the morphological analysis correlate well to the results of the luciferase assay (Figs. 4 and 5).

C2C12 cells were seeded on hydrogel samples with different combinations of PEGDA to AA ratios and CMA. For all conditions, the cells survived and were metabolically active through 14 days, as shown in Fig. 6. Tissue culture polystyrene (TCP) was used as a positive control. TCP control group showed a significantly higher metabolic activity than all other groups at all time-points. The cells seeded on CMA + 1:4 PEGDA:AA and CMA + 1:8 PEGDA:AA hydrogel samples had a subtle increase in metabolic activity

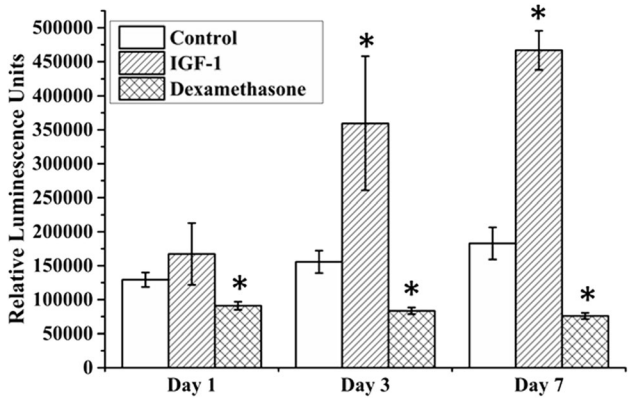

FIGURE 4. Cell line validation: luciferase assay. Luciferase assay performed on days 1, 3, and 7 after applying differentiation media in the validation of the cell line development.

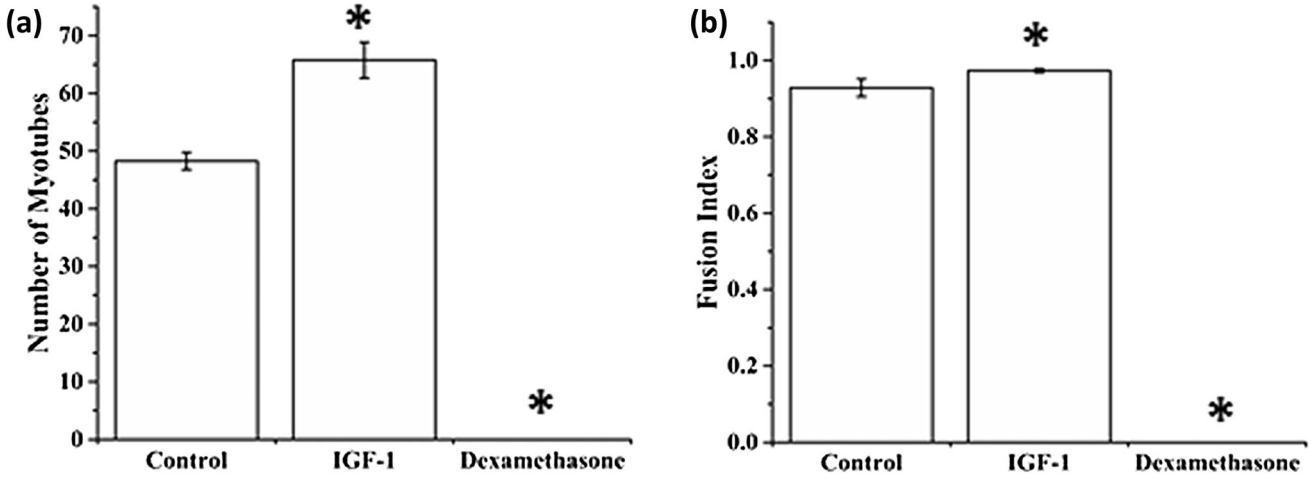

FIGURE 5. Cell line validation: morphological analysis. Morphological analysis of the myoblasts used in the validation of the cell line on day 7 after application of differentiation media. (a) Number of myotubes. (b) Fusion index.

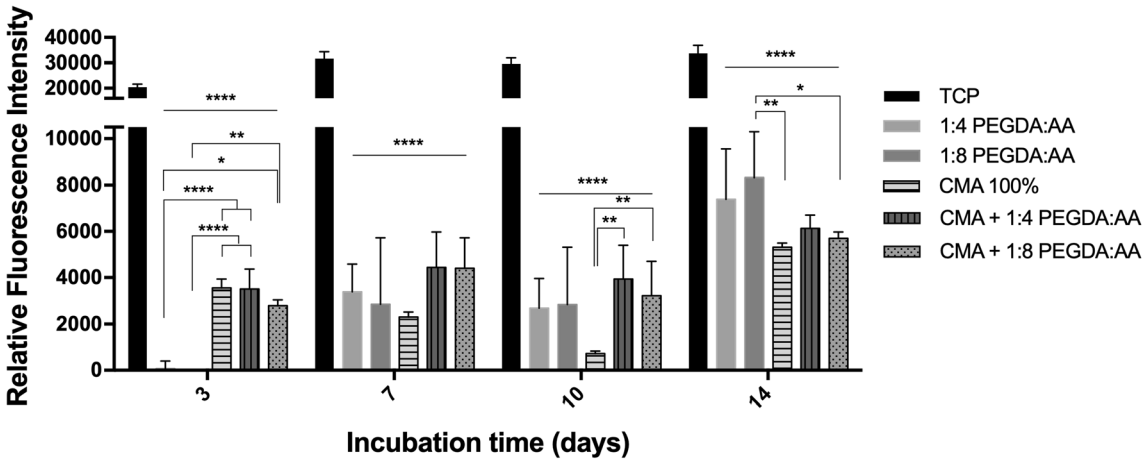

FIGURE 6. Metabolic activity data of C2C12 cells measured by a PrestoBlue® cell viability assay ($n = 4$). A statistical analysis performed by two-way ANOVA with a Tukey's *post hoc* test and confidence level of 95% ($\alpha = 0.05$) was conducted (*indicates a statistically significant difference between corresponding conditions). ****$p < 0.0001$, *$0.0001 < p < 0.001$, **$0.001 < p < 0.01$, and *$0.01 < p < 0.05$.**

throughout the 14 days, with a statistically significant increase from day 1 to day 14 for both conditions. For 1:4 PEGDA:AA and 1:8 PEGDA:AA hydrogel samples, an initial delay in metabolic activity was observed on day 3 where there is no metabolic activity detected, with a sudden increase at day 7 that continued to intensify throughout the incubation time. We hypothesize that this initial delay in metabolic activity is a result of the hostile environment driven by the direct exposure to AA that the cells had to endure. In contrast, all hydrogels with CMA were able to show some initial metabolic activity as CMA improved initial biocompatibility. Additionally, there was no dependence in AA concentration and metabolic activity on any of the time points for the PEGDA and CMA + PEGDA hydrogel samples. Although most groups had relatively constant or increasing metabolic activity throughout the study period, the 100% CMA group had a decrease in metabolic activity for the first 10 days of incubation with the lowest metabolic activity occurring on day 10 and a significant increase on day 14.

Cellular gene expression of MLC was assessed by using a cell line that links luciferase production to MLC. TCP, as a positive control, showed significantly higher gene expression compared to all other groups at all time-points (Fig. 7). On day 3, 1:4 PEGDA:AA and 1:8 PEGDA:AA hydrogel samples showed no MLC activity with a sudden increase for both AA concentrations at day 7. This level of activity remained consistent for 1:8 PEGDA:AA hydrogel but continued to intensify throughout day 14 for 1:4 PEGDA:AA

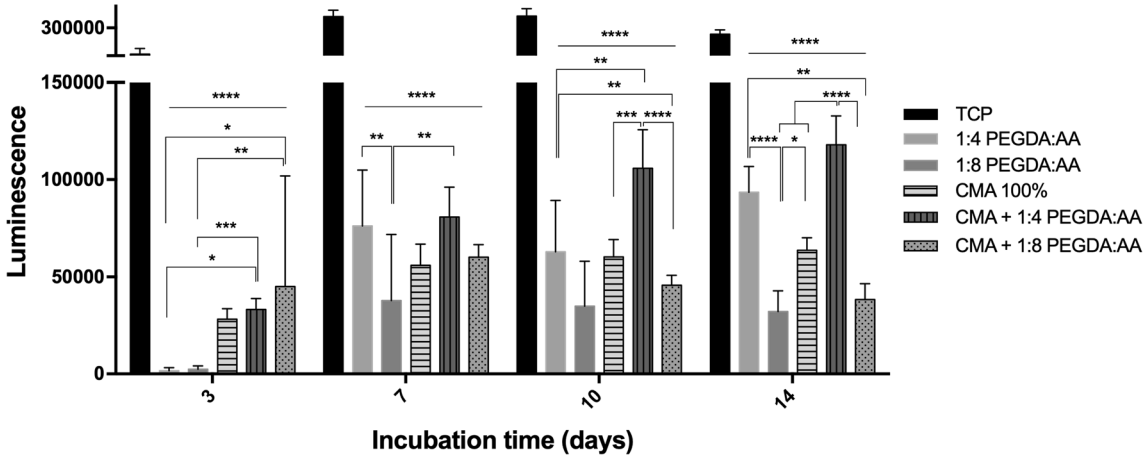

FIGURE 7. Myosin light chain expression measured by a Pierce™ Gaussia luciferase glow assay kit ($n = 4$). A statistical analysis performed by two-way ANOVA with a Tukey's *post hoc* test and confidence level of 95% ($\alpha = 0.05$) was conducted (*indicates a statistically significant difference between corresponding conditions). ****$p < 0.0001$, *$0.0001 < p < 0.001$, **$0.001 < p < 0.01$, and *$0.01 < p < 0.05$.**

hydrogel. CMA 100%, showed lower MLC activity, similar to CMA + 1:4 PEGDA: AA and CMA + 1:8 PEGDA:AA hydrogel samples for day 3 with a significant increase on day 7 that stayed constant all through day 14. Similarly, CMA + 1:4 PEGDA:AA and CMA + 1:8 PEGDA:AA hydrogel samples had an increase in metabolic activity on day 7 that was maintained on day 10 and further increased on day 14.

Cellular morphology and attachment were assessed by staining the cells with phalloidin to identify actin (green) and DAPI to identify DNA (blue) on day 14, as shown in Fig. 8. Cells were present for all hydrogel samples with distinctive variations in attachment, spreading, and growth. Cells seeded on TCP show a consistent high cell attachment throughout the 14 days of the study compared to all the different hydrogels. 1:8 PEGDA:AA and CMA + 1:8 PEGDA:AA hydrogels demonstrated the highest level of cell adhesion and intracellular matrix (actin) production, with some evidence of cell fusion. Addition of CMA to 1:8 PEGDA:AA hydrogels further led to extended, multinucleated structures, which can be considered a sign of myotube formation during differentiation. The 1:4 PEGDA:AA samples had reduced intracellular matrix production and lower cell attachment. The addition of CMA to 1:4 PEGDA:AA hydrogels, showed an increase in cell proliferation and fusion with evidence of intracellular matrix production. CMA hydrogels show enhanced cell proliferation and spreading.

Fusion Indices

The fusion indices for myoblasts on each hydrogel were calculated as a measure of cell differentiation after 14 days (Fig. 9). Significant differences in fusion index were founds between Control vs. PEGDA 1:4, CMA vs. PEGDA 1:4, CMA + PEGDA 1:4 vs. PEGDA 1:4, CMA + PEGDA 1:4 vs. PEGDA 1:4, and CMA + PEGDA 1:8 vs. PEGDA 1:4 (from ANOVA and *t*-test). The 1:4 PEGDA:AA samples displayed the lowest fusion index. PEGDA 1:8 displayed a higher fusion index than PEGDA 1:4 (from *t*-test). The control group (TCP) and the CMA alone also had a larger fusion index than 1:4 PEGDA:AA.

Cellular Live/Dead Assessment

In the cellular Live/Dead assay, all hydrogels exhibited an increase in viability with longer incubation times. On day 3, cellular distribution in TCP is uniform with a higher cellular survival rate. In comparison, 1:4 PEGDA:AA, CMA, and CMA + 1:8 PEGDA:AA showed reduced cell viability and distribution with formation of cellular clusters. In contrast, 1:8 PEGDA:AA and CMA + 1:4 PEGDA:AA showed increased cell viability and distribution. As the study progressed, we saw the impact of serum reduction in cell differentiation. From day 0 to day 7, cells were cultured in serum rich media with 10% FBS allowing them to grow and multiply. From day 7 to day 14, FBS was reduced to 1% to encourage differentiation. Furthermore, we observe how the addition of CMA creates extended cellular structures that the polymer alone does not achieve (Fig. 9). After 14 days of incubation, we observe myotube formation with early signs of cell differentiation where C2C12 myoblasts fuse together to form elongated, multinucleated structures resembling myotubes in TCP and 1:4 PEGDA:AA (Figs. 10 and 11). However, 1:8 PEGDA:AA, as well as all conditions with CMA failed to form myotubes.

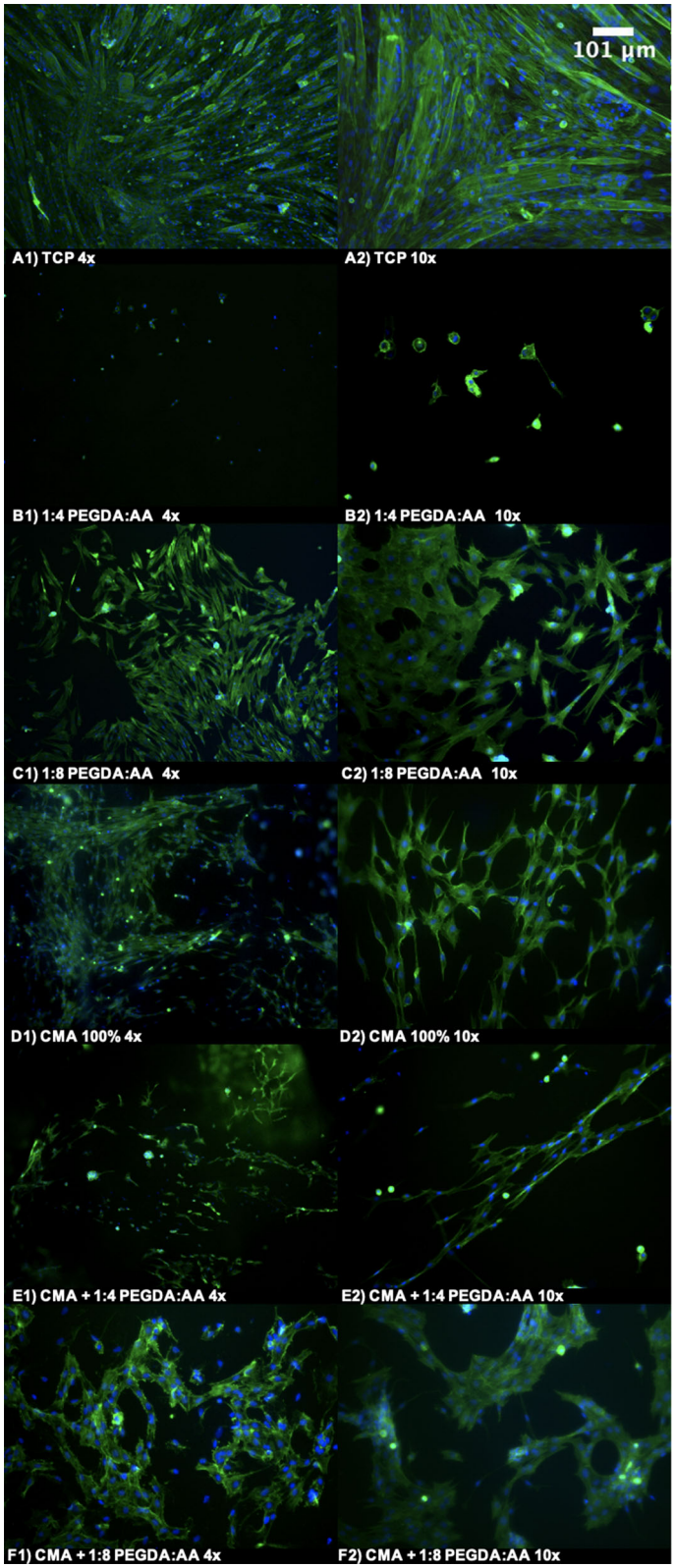

FIGURE 8. On day 14, cells were stained with phalloidin to identify actin (green) and with DAPI to identify DNA (blue) and imaged using a × 4 and × 10 objective, from left to right. (a1, a2) TCP. (b1, b2) 1:4 PEGDA:AA. (c1, c2) 1:8 PEGDA:AA. (d1, d2) CMA 100%. (e1, e2) CMA + 1:4 PEGDA:AA. (f1, f2) CMA + 1:8 PEGDA:AA.

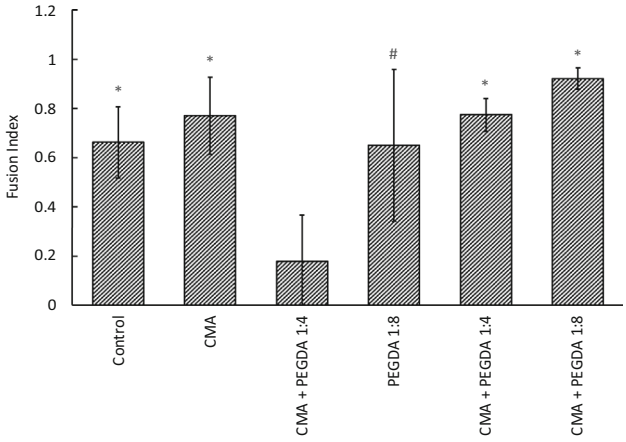

FIGURE 9. Fusion index from day 14 images of myoblasts stained with phalloidin to identify actin (green) and with DAPI to identify nuclei (blue) and imaged using a × 10 objective. Fusion index was calculated using the number of nuclei on myotubes/total number of nuclei. *Notes a significant difference vs. PEGDA 1:4 using ANOVA (with a Tukey's *post hoc* test) and *t*-test, #notes a significant difference vs. PEGDA 1:4 using *t*-test. Significance level for all analyses was $\alpha \leq 0.05$.

DISCUSSION

In this study, we first characterized the ability of PEGDA:AA hydrogels of different compositions to respond to an electric field. Two ratios of PEGDA:AA were used, with and without supplementation with CMA to improve biocompatibility. All hydrogel samples, in the shape of rectangular prisms, responded to the electric field stimulus through angular displacement (as noted previously by our group), which shows promise for applications as actuators.[8] In the presence of an ionic solution and an electrical stimulus, PEGDA is attracted to the cations from the solution. This attracts polar water molecules, causing one side of the polymer to swell and the other to shrink, which results in the bending of the hydrogel. The swelling density of the PEGDA:AA was previously determined to be proportional to AA concentration, where 1:4 PEGDA:AA increased to 150% of its original size while 1:8 PEGDA:AA increased 200% of its original size.[8] Due to the greater presence of anions in the polymer with the higher concentration of AA, the 1:8 PEGDA:AA hydrogel showed a higher degree of movement compared to the 1:4 PEGDA:AA construct. CMA + 1:8 PEGDA:AA hydrogels showed a significant reduction in actuation activity compared to 1:8 PEGDA:AA. Overall, the incorporation of CMA onto the PEGDA:AA (1:4 and 1:8) constructs reduced the movement of the scaffold due to hysteric hindrance. While we see a difference in the degree of interference with movement between the two ratios of PEGDA:AA (1:4 and 1:8), we attribute it to PEGDA:AA 1:8 having a higher concentration of charged ions.

For 1:4 PEGDA:AA hydrogels, the addition of CMA reduced with statistical significance the displacement in the forward direction while the displacement in reverse direction was maintained. Thus, the addition of CMA reduced actuation, possibly due to

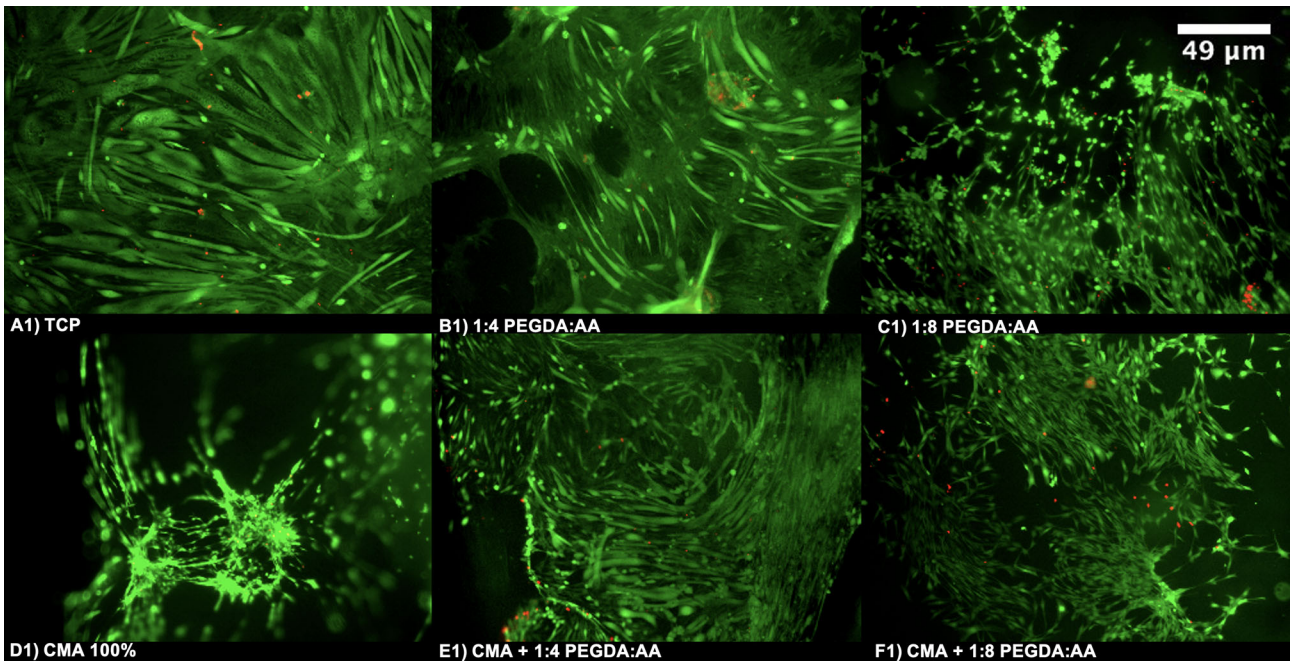

FIGURE 10. On day 14, cells were stained with calcein-AM (green) and ethidium homodimer-1 (red) to assess cytotoxicity and viability and imaged at × 4 magnification, from left to right. (a1) TCP. (b1) 1:4 PEGDA:AA. (c1) 1:8 PEGDA:AA. (d1) CMA 100%. (e1) CMA + 1:4 PEGDA:AA. (f1) CMA + 1:8 PEGDA:AA.

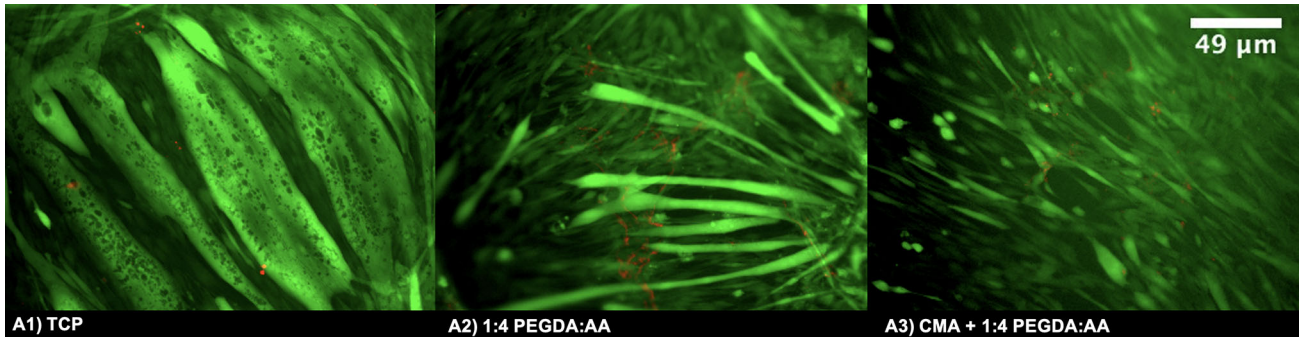

FIGURE 11. On day 14, cells were stained with calcein-AM (green) and ethidium homodimer-1 (red) to assess cytotoxicity and viability and imaged with a × 10 objective, from left to right. (a1) TCP. (a2) 1:4 PEGDA:AA. (a3) CMA + 1:4 PEGDA:AA.

steric hindrance or the presence of charged amino acids altering the movement of ions within the gel. Steric hindrance is more likely as the CMA and PEGDA most likely formed an interpenetrating network with the CMA crosslinks forming around the crosslinked PEGDA. Furthermore, the incorporation of CMA onto PEGDA hydrogels presented a challenge due to the viscous fluid like behavior that afforded non-homogeneous samples for actuation testing. For future studies, we would like to better incorporate CMA into PEGDA hydrogels to afford homogeneous samples.

Secondly, we aimed to characterize the biological properties of the materials *in vitro*. To that end, we carried out a 14-day cell study using C2C12 myoblast cells, analyzing the cells at 4 time points (day 3, 7, 10, and 14). At each time point, the metabolic activity of the cells incubated with the constructs and corresponding controls was assessed through a PrestoBlue assay. As the PrestoBlue cell viability reagent enters the cytosol of living cells, it is reduced resulting in a color change that can be measured through a fluorescent readout. This indicator dye only changes color as metabolically-active cells reduce it, where the higher the fluorescence detected, the higher cellular metabolic activity. C2C12 cells seeded in both PEGDA:AA hydrogels showed similar metabolic activity, with no significant influence of AA concentration. We found that CMA has an innate opaqueness that affects the fluorescence intensity measured of the cells on the hydrogel. Thus, to have a better understanding of the cell behavior for each time point the images were analyzed together with the cell assay results. The addition of CMA increased the metabolic activity of the cells. As an essential component of the muscle extracellular matrix (ECM), collagen type-I participates in muscle regeneration to provide structural support and biological cues that enhance cellular activity.[39] CMA alone showed a reduction in cellular metabolic activity when compared to PEGDA:AA hydrogels and CMA + PEGDA:AA hydrogels. This is due to the limited mechanical support that CMA would provide compared to PEGDA:AA, which has higher stiffness.[19,23]

The gene expression of MLC was also measured during each time point using a cell line that relates luciferase production to MLC expression. During initial incubation, all conditions showed reduced MLC expression. However, at later time points we observe an increase in MLC expression, which can be attributed to initial signs of differentiation.[21] In addition, we observe a significant increase in MLC expression for 1:4 PEGDA:AA and CMA + 1:4 PEGDA:AA groups. Thus, to further validate this system, 1:4 will be the preferred PEGDA:AA ratio due to higher MLC expression. The increase of MLC expression, as a marker of myoblast expression, shows that the polymer in the presence of CMA is enhancing differentiation and potential muscle development relative to the PEGDA hydrogels without CMA. This can be attributed to the high prevalence of collagen in muscle, which is one of the most favorable biomaterials for muscle development. Additionally, the presence of collagen type I has been shown to promote the myogenic differentiation of the C2C12 cells, which in turn would increase the MLC expression as seen above.[39] Although MLC expression results does not appear to support the observation that C2C12 myoblasts are differentiating on the substrates under study, the myotube fusion results suggest otherwise.

Finally, the cells were imaged at all time points using immunofluorescence staining (DAPI and phalloidin) and cell viability was assessed utilizing Live/Dead staining following the methodology of our previous published studies.[8] C2C12 myogenic differentiation was achieved through serum deprivation halfway (day 7) through the *in vitro* study. In the first days of incubation, we assessed how cell shape and orientation is influenced by the presence of CMA. Cells seeded on PEGDA:AA hydrogels spread out in an isotropic manner, whereas cells seeded on CMA hydrogels and

CMA coated hydrogels cells aligned along one direction with a spindle-like shape. These findings suggest that the collagen fibers influence the direction and shape of the C2C12 cells due to substrate topography-based behavior, which follows the principle of contact guidance.[11] The collagen gives the cells the amino acid sequences that are necessary for binding to the sample. In the last day of incubation in the Live/Dead stained cultures we see multinucleated myotube formation from the fusion of C2C12 cells cultured in differentiation medium for TCP and on 1:4 PEGDA:AA hydrogels. C2C12 cells seeded on 1:8 PEGDA:AA hydrogels failed to form elongated linear myotubes due to the lack of guidance cues in the hydrogel surface which would result in attachment and fusion support. Hydrogels with CMA improved cell proliferation with distinguishable extended, multinucleated structures. The development of these multinucleated structures could be a possible sign of myotube formation during differentiation.

To show events of cell–cell fusion during myogenesis the fusion index of C2C12 cells was measured after incubation with different combinations of PEGDA and CMA hydrogels.[1] Due to the nature of the materials under study, we expected limited myotube alignment given that the hydrogels are too soft. Upon further analysis, the addition of CMA to PEGDA 1:4 displayed an increase in fusion index. The addition of more AA (1:8 PEGDA:AA) also increased the fusion index. As the fusion index is a measure of myotube formation, the data seems to show that the addition of CMA improves myoblast differentiation. One caveat of our chosen method of image processing is that it is difficult to distinguish between non-myotube cells and myotubes. Myotubes are long striated cylindrical in morphology however there are cells that have continuous actin and nuclei however they are flattened out like pancakes or more trembling of fibroblasts with bipolar morphology that has significant variation in cytoskeletal thickness from one nuclei to the next. Due to the definition of a myotube used in this study these cells could be counted in the processing as myotubes even though they are not in fact myotubes inflating the number of myotubes in that image. Groups where this occurred were CMA + PEGDA 1:4 and CMA + PEGDA 1:8. It is possible that the CMA is providing attachment for the cells to contract the material while the PEGDA which does not contain attachment sites prevents some adjacent cells to fuse and form tube-like structures. It is well known that contraction occurs within collagen-based materials when cells are grown on top/within them. Perhaps the collagen becomes contracted resulting in deformation of the overall matrix and bulging that disrupts or prevents cell–cell contact from occurring. This would explain why this did not take place in CMA samples. In our previous peer reviewed article, Browe *et al*. discusses an in-depth characterization of PEGDA:AA hydrogels to support the process of myogenesis.[8]

Future work will focus on increasing the blending of the two materials to enhance cell adhesion, alignment, and myoblast fusion. We could also decrease the amount of CMA added to maintain increased bioactivity while decreasing potential hindrance to actuation. The PEGDA could be altered to include groups for cell binding such as RGD sequences or amine groups. The molecular weight of the PEGDA could also be altered in order to increase the density of PEGDA:AA to increase movement even after CMA is added.

Conclusion

In muscle tissue engineering, EAPs such as polyethylene glycol diacrylate–acrylic acid (PEGDA:AA) show promise as they can stimulate cells through mechanical, electrical, and topographical cues.[8] In this study, we showed that the addition of a bioactive and photoactive polymer like CMA onto actuating PEGDA:AA scaffolds enhance the biological properties of this electroactive system. The AA ratio 1:4 PEGDA:AA was able to better perform in combination with CMA as it responded to an electric field stimulus through angular displacement. Moreover, 1:4 PEGDA:AA + CMA scaffolds improved cell proliferation with distinguishable extended, multinucleated structures and increased MLC expression. Unfortunately, the addition of CMA also decreased the amount of sample actuation. Future studies will evaluate the relationship between the amount of CMA added and the sample actuation and biocompatibility. During actuation we will also examine actuation using lower voltages with shorter distances between electrodes to create a system that is more conducive to cell survival. Additionally, actuation studies with cells seeded on the hydrogel are also encouraged for future work.

The outcomes of this study support the idea that CMA, in conjunction with actuating polymers, can be added to our library of EAPs to fabricate contractile muscle scaffolds. Although the amount of actuation was reduced, altering the formulation may counter this effect. Thus, bioactive polymers combined with conductive materials can afford the creation of scaffolds that can contract and expand to generate force while regenerating muscle *in vivo*.

The CMA and PEGDA:AA hydrogel composite is a mechanically dynamic, and bioactive hydrogel allows for the development of soft-tissue scaffolds with a range of stiffnesses allowed from non-crosslinked to crosslinked regions affording diverse mechanical

microenvironments.[23] Alterations in the stiffness of the microenvironments through percent crosslinking of the CMA may influence the myogenic differentiation of the progenitor cells. Exploring how stiffness of CMA influences differentiation of the progenitor cells may yield insights as to which conditions provide with most favorable environmental parameters to produce these scaffolds for muscle regeneration that not only influence differentiation but also proliferation of cells within them.[61] This could be accomplished by tuning the crosslinking of CMA as well as exploring other ratios of CMA:PEGDA/AA.

CONFLICT OF INTEREST

No benefits in any form have been or will be received from a commercial party related directly or indirectly to the subject of this manuscript.

REFERENCES

[1]Agley, C. C., C. P. Velloso, N. R. Lazarus, and S. D. Harridge. An image analysis method for the precise selection and quantitation of fluorescently labeled cellular constituents: application to the measurement of human muscle cells in culture. *J. Histochem. Cytochem.* 60(6):428–438, 2012. https://doi.org/10.1369/0022155412442897.

[2]Apsite, I., J. M. Uribe, A. F. Posada, S. Rosenfeldt, S. Salehi, and L. Ionov. 4D biofabrication of skeletal muscle microtissues. *Biofabrication*.12:015016, 2019.

[3]Bach, A. D., J. P. Beier, J. Stern-Staeter, and R. E. Horch. Skeletal muscle tissue engineering. *J. Cell. Mol. Med.* 8(4):413–422, 2004.

[58]Bar-Cohen, Y. Electroactive polymer (EAP) actuators as artificial muscles: reality, potential, and challenges, 2nd ed. Bellingham, WA: SPIE Press, p. xvii, 2004.

[5]Bar-Cohen, Y. Electroactive polymers as an enabling materials technology. *Proc. Inst. Mech. Eng. G.* 221(4):553–564, 2007.

[6]Bauer, A., L. Gu, B. Kwee, W. A. Li, M. Dellacherie, A. D. Celiz, et al. Hydrogel substrate stress-relaxation regulates the spreading and proliferation of mouse myoblasts. *Acta Biomater.* 62:82–90, 2017.

[7]Beier, J. P., J. Stern-Straeter, V. T. Foerster, U. Kneser, G. B. Stark, and A. D. Bach. Tissue engineering of injectable muscle: three-dimensional myoblast-fibrin injection in the syngeneic rat animal model. *Plast. Reconstr. Surg.* 118(5):1113–1121, 2006.

[8]Browe, D. P., C. Wood, M. T. Sze, K. A. White, T. Scott, R. M. Olabisi, et al. Characterization and optimization of actuating poly(ethylene glycol) diacrylate/acrylic acid hydrogels as artificial muscles. *Polymer.* 117:331–341, 2017.

[9]Cai, A., M. Hardt, P. Schneider, R. Schmid, C. Lange, D. Dippold, et al. Myogenic differentiation of primary myoblasts and mesenchymal stromal cells under serum-free conditions on PCL–collagen I-nanoscaffolds. *BMC Biotechnol.* 18(1):1–12, 2018.

[10]Chaturvedi, V., D. Naskar, B. F. Kinnear, E. Grenik, D. E. Dye, M. D. Grounds, et al. Silk fibroin scaffolds with muscle-like elasticity support in vitro differentiation of human skeletal muscle cells. *J. Tissue Eng. Regen. Med.* 11:3178–3192, 2017.

[11]Chaubaroux, C., F. Perrin-Schmitt, B. Senger, L. Vidal, J. C. Voegel, P. Schaaf, et al. Cell alignment driven by mechanically induced collagen fiber alignment in collagen/alginate coatings. *Tissue Eng. C.* 21(9):881–888, 2015.

[12]Chen, S., T. Nakamoto, N. Kawazoe, and G. Chen. Engineering multi-layered skeletal muscle tissue by using 3D microgrooved collagen scaffolds. *Biomaterials.* 73:23–31, 2015. https://doi.org/10.1016/j.biomaterials.2015.09.010.

[13]Choi, Y. J., Y. J. Jun, D. Y. Kim, H. G. Yi, S. H. Chae, J. Kang, et al. A 3D cell printed muscle construct with tissue-derived bioink for the treatment of volumetric muscle loss. *Biomaterials.* 206:160–169, 2019.

[14]Choi, Y. J., T. G. Kim, J. Jeong, H. G. Yi, J. W. Park, W. Hwang, et al. 3D cell printing of functional skeletal muscle constructs using skeletal muscle-derived bioink. *Adv. Healthc. Mater.* 5(20):2636–2645, 2016.

[15]Clark, M. E. editor Pain issues among OEF and OIF returnees. In: *VA/DOD Emerging Concepts Conference*, 2007, Las Vegas, NV.

[16]De Deyne, P. G. Formation of sarcomeres in developing myotubes: role of mechanical stretch and contractile activation. *Am. J. Physiol. Cell Physiol.* 279(6):C1801–C1811, 2000.

[17]De Santis, M. M., H. N. Alsafadi, S. Tas, D. A. Bolukbas, S. Prithiviraj, I. A. N. Da Silva, et al. Extracellular-matrix-reinforced bioinks for 3D bioprinting human tissue. *Adv. Mater.*33:e2005476, 2021.

[18]Denes, L. T., L. A. Riley, J. R. Mijares, J. D. Arboleda, K. McKee, K. A. Esser, et al. Culturing C2C12 myotubes on micromolded gelatin hydrogels accelerates myotube maturation. *Skelet. Muscle.* 9(1):17, 2019.

[19]Drzewiecki, K. E., A. S. Parmar, I. D. Gaudet, J. R. Branch, D. H. Pike, V. Nanda, et al. Methacrylation induces rapid, temperature-dependent, reversible self-assembly of type-I collagen. *Langmuir.* 30(37):11204–11211, 2014.

[20]Fujita, H., T. Nedachi, and M. Kanzaki. Accelerated de novo sarcomere assembly by electric pulse stimulation in C2C12 myotubes. *Exp. Cell Res.* 313(9):1853–1865, 2007.

[21]Fujita, H., K. Shimizu, and E. Nagamori. Novel method for fabrication of skeletal muscle construct from the C2C12 myoblast cell line using serum-free medium AIM-V. *Biotechnol. Bioeng.* 103(5):1034–1041, 2009.

[22]Garcia-Lizarribar, A., X. Fernandez-Garibay, F. Velasco-Mallorqui, A. G. Castano, J. Samitier, and J. Ramon-Azcon. Composite biomaterials as long-lasting scaffolds for 3D bioprinting of highly aligned muscle tissue. *Macromol. Biosci.*18:e1800167, 2018.

[23]Gaudet, I. D., and D. I. Shreiber. Characterization of methacrylated type-I collagen as a dynamic, photoactive hydrogel. *Biointerphases.* 7(1–4):25, 2012.

[24]Gong, H. Y., J. Park, W. Kim, J. Kim, J. Y. Lee, and W. G. Koh. A novel conductive and micropatterned PEG-based hydrogel enabling the topographical and electrical stimulation of myoblasts. *ACS Appl. Mater. Interfaces.* 11:47695–47706, 2019.

[25]Gribova, V., C. Y. Liu, A. Nishiguchi, M. Matsusaki, T. Boudou, C. Picart, et al. Construction and myogenic differentiation of 3D myoblast tissues fabricated by fi-

bronectin–gelatin nanofilm coating. *Biochem. Biophys. Res. Commun*. 474:515–521, 2016.
[26]Hill, E., T. Boontheekul, and D. J. Mooney. Designing scaffolds to enhance transplanted myoblast survival and migration. *Tissue Eng*. 12:1295–1304, 2006.
[27]Hitti, M. *Report: Nearly 5.6 Million Americans Paralyzed: Web MD*, 2009.
[28]Iyer, S. R., N. Udpa, and Y. Gao. Chitosan selectively promotes adhesion of myoblasts over fibroblasts. *J. Biomed. Mater. Res. A*. 103:1899–1906, 2015.
[29]Jo, H., M. Sim, S. Kim, S. Yang, Y. Yoo, J. H. Park, et al. Electrically conductive graphene/polyacrylamide hydrogels produced by mild chemical reduction for enhanced myoblast growth and differentiation. *Acta Biomater*. 48:100–109, 2017.
[30]Joglekar, D., R. Warren, D. Browe, E. Ekwueme, M. Dariani, N. D. Padliya, et al. Investigating the effects of fertilized egg yolk extract on myoblast proliferation and differentiation. *Regen. Eng. Transl. Med*. 6:125–137, 2020.
[31]Kim, W., C. H. Jang, and G. H. Kim. A myoblast-laden collagen bioink with fully aligned Au nanowires for muscle-tissue regeneration. *Nano Lett*. 19:8612–8620, 2019.
[32]Kim, W., H. Lee, J. Lee, A. Atala, J. J. Yoo, S. J. Lee, et al. Efficient myotube formation in 3D bioprinted tissue construct by biochemical and topographical cues. *Biomaterials*.230:119632, 2020.
[33]Ko, U. H., S. Park, H. Bang, M. Kim, H. Shin, and J. H. Shin. Promotion of myogenic maturation by timely application of electric field along the topographical alignment. *Tissue Eng. A*. 24:752–760, 2018.
[34]Kung, F. H., D. Sillitti, A. B. Shrirao, D. I. Shreiber, and B. L. Firestein. Collagen nanofibre anisotropy induces myotube differentiation and acetylcholine receptor clustering. *J. Tissue Eng. Regen. Med*. 12:e2010–e2019, 2018.
[35]Lee, H., W. Kim, J. Lee, J. J. Yoo, G. H. Kim, and S. J. Lee. Effect of hierarchical scaffold consisting of aligned dECM nanofibers and poly(lactide-*co*-glycolide) struts on the orientation and maturation of human muscle progenitor cells. *ACS Appl. Mater. Interfaces*. 11:39449–39458, 2019.
[36]Levett, P. A., F. P. W. Melchels, K. Schrobback, D. W. Hutmacher, J. Malda, and T. J. Klein. A biomimetic extracellular matrix for cartilage tissue engineering centered on photocurable gelatin, hyaluronic acid and chondroitin sulfate. *Acta Biomater*. 10(1):214–223, 2014. https://doi.org/10.1016/j.actbio.2013.10.005.
[37]Li, R., N. L. McRae, D. R. McCulloch, M. Boyd-Moss, C. J. Barrow, D. R. Nisbet, et al. Large and small assembly: combining functional macromolecules with small peptides to control the morphology of skeletal muscle progenitor cells. *Biomacromolecules*. 19:825–837, 2018.
[38]Liao, I. C., J. B. Liu, N. Bursac, and K. W. Leong, editors. Effect of electromechanical stimulation on the maturation of myotubes on aligned electrospun fibers. In: Annual Meeting of the Biomedical-Engineering-Society, 2 Oct 2008, St Louis, MO, 2008.
[39]Liu, X., Y. Gao, X. Long, T. Hayashi, K. Mizuno, S. Hattori, et al. Type I collagen promotes the migration and myogenic differentiation of C2C12 myoblasts via the release of interleukin-6 mediated by FAK/NF-κB p65 activation. *Food Funct*. 11(1):328–338, 2020.
[40]Lumia, R., and M. Shahinpoor. IPMC microgripper research and development. *J. Phys. Conf. Ser*. 127(1):1–15, 2008.
[41]Manchineella, S., G. Thrivikraman, K. K. Khanum, P. C. Ramamurthy, B. Basu, and T. Govindaraju. Pigmented silk nanofibrous composite for skeletal muscle tissue engineering. *Adv. Healthc. Mater*. 5:1222–1232, 2016.
[42]Markert, C. D., A. Atala, J. K. Cann, G. Christ, M. Furth, F. Ambrosio, et al. Mesenchymal stem cells: emerging therapy for Duchenne muscular dystrophy. *PM&R*. 1(6):547–559, 2009.
[43]Mazzoccoli, J. P., D. L. Feke, H. Baskaran, and P. N. Pintauro. Mechanical and cell viability properties of crosslinked low- and high-molecular weight poly (ethylene glycol) diacrylate blends. *J. Biomed. Mater. Res. A*. 93(2):558–566, 2010.
[44]Meriggioli, M. N., and D. B. Sanders. Autoimmune myasthenia gravis: emerging clinical and biological heterogeneity. *Lancet Neurol*. 8(5):475–490, 2009.
[45]Nagai, Y., H. Yokoi, K. Kaihara, and K. Naruse. The mechanical stimulation of cells in 3D culture within a self-assembling peptide hydrogel. *Biomaterials*. 33:1044–1051, 2012.
[46]Narayanan, N., Z. Jia, K. H. Kim, L. Kuang, P. Lengemann, G. Shafer, et al. Biomimetic glycosaminoglycan-based scaffolds improve skeletal muscle regeneration in a murine volumetric muscle loss model. *Bioact. Mater*. 6:1201–1213, 2021.
[47]Narayanan, N., C. Jiang, C. Wang, G. Uzunalli, N. Whittern, D. Chen, et al. Harnessing fiber diameter-dependent effects of myoblasts toward biomimetic scaffold-based skeletal muscle regeneration. *Front. Bioeng. Biotechnol*. 8:203, 2020.
[48]Neuhaus, R., N. Zahiri, J. Petrs, et al. Integrating ionic electroactive polymer actuators and sensors into adaptive building skins—potentials and limitations. *Front. Built Environ*. 2020. https://doi.org/10.3389/fbuil.2020.00095.
[49]Ngan, C., A. Quigley, C. O'Connell, M. Kita, J. Bourke, G. G. Wallace, et al. 3D bioprinting and differentiation of primary skeletal muscle progenitor cells. *Methods Mol. Biol*. 2140:229–242, 2020.
[50]Ostrovidov, S., S. Ahadian, J. Ramon-Azcon, V. Hosseini, T. Fujie, S. P. Parthiban, et al. Three-dimensional co-culture of C2C12/PC12 cells improves skeletal muscle tissue formation and function. *J. Tissue Eng. Regen. Med*. 11:582–595, 2017.
[51]Ostrovidov, S., X. Shi, L. Zhang, X. Liang, S. B. Kim, T. Fujie, et al. Myotube formation on gelatin nanofibers–multi-walled carbon nanotubes hybrid scaffolds. *Biomaterials*. 35:6268–6277, 2014.
[52]Pankongadisak, P., E. Tsekoura, O. Suwantong, and H. Uludag. Electrospun gelatin matrices with bioactive pDNA polyplexes. *Int. J. Biol. Macromol*. 149:296–308, 2020.
[53]Park, J., J. H. Choi, S. Kim, I. Jang, S. Jeong, and J. Y. Lee. Micropatterned conductive hydrogels as multifunctional muscle-mimicking biomaterials: graphene-incorporated hydrogels directly patterned with femtosecond laser ablation. *Acta Biomater*. 97:141–153, 2019.
[54]Patel, K. H., A. J. Dunn, M. Talovic, G. J. Haas, M. Marcinczyk, H. Elmashhady, et al. Aligned nanofibers of decellularized muscle ECM support myogenic activity in primary satellite cells in vitro. *Biomed. Mater*.14:035010, 2019.
[55]Patel, A., S. Vendrell-Gonzalez, G. Haas, M. Marcinczyk, N. Ziemkiewicz, M. Talovic, et al. Regulation of myogenic activity by substrate and electrical stimulation in vitro. *BioResearch Open Access*. 8:129–138, 2019.

[56]Pollot, B. E., C. R. Rathbone, J. C. Wenke, and T. Guda. Natural polymeric hydrogel evaluation for skeletal muscle tissue engineering. *J. Biomed. Mater. Res. B.* 106:672–679, 2018.
[57]Porzionato, A., M. M. Sfriso, A. Pontini, V. Macchi, L. Petrelli, P. G. Pavan, et al. Decellularized human skeletal muscle as biologic scaffold for reconstructive surgery. *Int. J. Mol. Sci.* 16:14808–14831, 2015.
[58]Pruller, J., I. Mannhardt, T. Eschenhagen, P. S. Zammit, and N. Figeac. Satellite cells delivered in their niche efficiently generate functional myotubes in three-dimensional cell culture. *PLoS ONE*.13:e0202574, 2018.
[59]Punga, A. R., and M. A. Ruegg. Signaling and aging at the neuromuscular synapse: lessons learnt from neuromuscular diseases. *Curr. Opin. Pharmacol.* 12(3):340–346, 2012.
[60]Rando, T. A. Non-viral gene therapy for Duchenne muscular dystrophy: progress and challenges. *Biochim. Biophys. Acta Mol. Basis Dis.* 1772(2):263–271, 2007.
[61]Romanazzo, S., G. Forte, M. Ebara, K. Uto, S. Pagliari, T. Aoyagi, et al. Substrate stiffness affects skeletal myoblast differentiation in vitro. *Sci. Technol. Adv. Mater*.13(6):064211, 2012.
[62]Rowley, J. A., and D. J. Mooney. Alginate type and RGD density control myoblast phenotype. *J. Biomed. Mater. Res.* 60:217–223, 2002.
[63]Scott, T. E., A. Khalili, B. Newton, R. Warren, D. P. Browe, and J. W. Freeman. Characterization and optimization of a positively charged poly(ethylene glycol) diacrylate hydrogel as an actuating muscle tissue engineering scaffold. *Polym. Adv. Technol.* 30(10):2604–2612, 2019.
[64]Serena, E., M. Flaibani, S. Carnio, L. Boldrin, L. Vitiello, P. De Coppi, et al. Electrophysiologic stimulation improves myogenic potential of muscle precursor cells grown in a 3D collagen scaffold. *Neurol. Res.* 30:207–214, 2008.
[65]Somers, S. M., N. Y. Zhang, J. B. F. Morrissette-McAlmon, K. Tran, H. Q. Mao, and W. L. Grayson. Myoblast maturity on aligned microfiber bundles at the onset of strain application impacts myogenic outcomes. *Acta Biomater.* 94:232–242, 2019.
[66]Ungerleide, J. L., T. D. Johnson, N. Rao, and K. L. Christman. Fabrication and characterization of injectable hydrogels derived from decellularized skeletal and cardiac muscle. *Methods.* 84:53–59, 2015.
[67]Ungerleider, J. L., T. D. Johnson, M. J. Hernandez, D. I. Elhag, R. L. Braden, M. Dzieciatkowska, et al. Extracellular matrix hydrogel promotes tissue remodeling, arteriogenesis, and perfusion in a rat hindlimb ischemia model. *JACC Basic Transl. Sci.* 1(1–2):32–44, 2016.
[68]Vartanian, A. D., A. Audfray, B. A. Jaam, M. Janot, S. Legardinier, A. Maftah, et al. Protein O-fucosyltransferase 1 expression impacts myogenic C2C12 cell commitment via the Notch signaling pathway. *Mol. Cell. Biol.* 35(2):391–405, 2015.
[69]Venugopal, J., L. L. Ma, T. Yong, and S. Ramakrishna. In vitro study of smooth muscle cells on polycaprolactone and collagen nanofibrous matrices. *Cell Biol. Int.* 29(10):861–867, 2005. https://doi.org/10.1016/j.cellbi.2005.03.026.
[70]Villanueva, P., S. Pereira, A. Olmo, P. Perez, Y. Yuste, A. Yufera, et al. Electrical pulse stimulation of skeletal myoblasts cell cultures with simulated action potentials. *J. Tissue Eng. Regen. Med.* 13:1265–1269, 2019.
[71]Wagner, K. R., N. Lechtzin, and D. P. Judge. Current treatment of adult Duchenne muscular dystrophy. *Biochim. Biophys. Acta Mol. Basis Dis.* 1772(2):229–237, 2007.
[72]Wang, W., M. Fan, L. Zhang, S. H. Liu, L. Sun, and C. Y. Wang. Compatibility of hyaluronic acid hydrogel and skeletal muscle myoblasts. *Biomed. Mater*.4:025011, 2009.
[73]Willmann, R., S. Possekel, J. Dubach-Powell, T. Meier, and M. A. Ruegg. Mammalian animal models for Duchenne muscular dystrophy. *Neuromuscul. Disord.* 19(4):241–249, 2009.
[74]Yeo, M., and G. Kim. Nano/microscale topographically designed alginate/PCL scaffolds for inducing myoblast alignment and myogenic differentiation. *Carbohydr. Polym*.223:115041, 2019.
[75]Yeo, M., and G. Kim. Micro/nano-hierarchical scaffold fabricated using a cell electrospinning/3D printing process for co-culturing myoblasts and HUVECs to induce myoblast alignment and differentiation. *Acta Biomater.* 107:102–114, 2020.
[76]Zhang, J., Z. Q. Hu, N. J. Turner, S. F. Teng, W. Y. Cheng, H. Y. Zhou, et al. Perfusion-decellularized skeletal muscle as a three-dimensional scaffold with a vascular network template. *Biomaterials.* 89:114–126, 2016.